

# Solutions of Conformal Israel-Stewart Relativistic Viscous Fluid Dynamics

Hugo Marrochio,<sup>1</sup> Jorge Noronha,<sup>1</sup> Gabriel S. Denicol,<sup>2</sup> Matthew Luzum,<sup>2,3</sup> Sangyong Jeon,<sup>2</sup> and Charles Gale<sup>2</sup>

<sup>1</sup>*Instituto de Física, Universidade de São Paulo, C.P. 66318, 05315-970 São Paulo, SP, Brazil*

<sup>2</sup>*Department of Physics, McGill University, 3600 University Street, Montreal, QC, H3A 2T8, Canada*

<sup>3</sup>*Lawrence Berkeley National Laboratory, Nuclear Science Division, MS 70R0319, Berkeley, CA 94720, USA*

We use symmetry arguments developed by Gubser to construct the first radially-expanding explicit solutions of the Israel-Stewart formulation of hydrodynamics. Along with a general semi-analytical solution, an exact analytical solution is given which is valid in the cold plasma limit where viscous effects from shear viscosity and the relaxation time coefficient are important. The radially expanding solutions presented in this paper can be used as nontrivial checks of numerical algorithms employed in hydrodynamic simulations of the quark-gluon plasma formed in ultra-relativistic heavy ion collisions. We show this explicitly by comparing such analytic and semi-analytic solutions with the corresponding numerical solutions obtained using the MUSIC viscous hydrodynamics simulation code.

PACS numbers: 12.38.Mh, 47.75.+f, 47.10.ad, 11.25.Hf

## I. INTRODUCTION

Our current understanding of the novel properties displayed by the Quark-Gluon Plasma (QGP) formed in ultra-relativistic heavy ion collisions [1] relies heavily on solving relativistic dissipative fluid dynamics [2, 3]. The equations of relativistic fluid dynamics form a set of complicated nonlinear partial differential equations, describing the conservation of energy-momentum and a conserved charge (such as net baryon number),

$$\partial_\mu T^{\mu\nu} = 0, \quad \partial_\mu N^\mu = 0.$$

In the presence of dissipation, the above equations are not closed and have to be supplemented by nine additional equations of motion, i.e., the time evolution equations for the bulk viscous pressure, heat flow, and shear-stress tensor.

The simplest formulation of relativistic dissipative fluid dynamics are the Navier-Stokes equations. However, due to instabilities and acausal signal propagation in these equations [4], they are not usually used in numerical simulations. Currently, most fluid-dynamical simulations of the QGP employ the relaxation-type equations derived by Israel and Stewart [5] to close the conservation laws. While some analytic solutions of the non-relativistic Navier-Stokes equations are widely known [6], very few analytical (or semi-analytical) solutions of relativistic fluid dynamics [7–10] have been obtained and most simulations of heavy ion collisions solve dissipative fluid dynamics numerically. Clearly, it would be useful to have solutions of Israel-Stewart theory in any limit, especially in the cases relevant to heavy ion collision applications.

In Refs. [11, 12], Gubser and Yarom derived  $SO(3) \otimes SU(1, 1) \otimes Z_2$  invariant solutions of ideal relativistic conformal fluid dynamics and relativistic Navier-Stokes theory. In this paper we use the same symmetry arguments to derive solutions of Israel-Stewart theory, which can be relevant to the description of the QGP. Like the well known Bjorken solution [7], the fluid dynamic variables in the dissipative solutions we obtain are invariant under Lorentz boosts in one direction, and are appropriate for comparison to data from heavy-ion collisions near mid-rapidity, which are approximately invariant under limited boosts in the beam direction. However, unlike the Bjorken solution, they also have nontrivial radial expansion.

Thus, the solutions found in this paper provide the most rigorous tests to date for the current numerical algorithms used to solve the viscous relativistic fluid dynamic equations in heavy ion collisions. We show this explicitly by comparing multi-dimensional numerical solutions obtained using MUSIC, a 3+1D viscous hydrodynamics simulation code [13], with the analytical and semi-analytical solutions of Israel-Stewart-like theories undergoing Gubser flow. We remark that the version of MUSIC employed in this work is an updated version currently being maintained at McGill University.

This paper is organized as follows. In the next section we briefly introduce the equations of relativistic dissipative fluid dynamics and describe the solution for the flow velocity obtained by Gubser. In Sec. III we derive the main results of this paper and solve the equations of motion of Israel-Stewart theory undergoing Gubser flow. We show in Sec. IV how these solutions can be used to test numerical simulations of relativistic fluid dynamics. We conclude with a summary of our results.

## II. HYDRODYNAMICS FOR HEAVY ION COLLISIONS AND GUBSER FLOW

In ultra-relativistic heavy ion applications, relativistic fluid dynamics is more naturally described in hyperbolic coordinates  $x^\mu = (\tau, r, \phi, \xi)$  where the line element is  $ds^2 = -d\tau^2 + dr^2 + r^2 d\phi^2 + \tau^2 d\xi^2$ ,  $r = \sqrt{x^2 + y^2}$ , and  $\phi$  parametrize the transverse plane perpendicular to the beam direction, while  $\tau = \sqrt{t^2 - z^2}$  and the rapidity  $\xi = 1/2 \times \ln[(t+z)/(t-z)]$  are given in terms of usual coordinates  $t$  and the beam direction  $z$ .

The minimum set of relaxation-type equations for a viscous conformal fluid is [14]

$$\frac{D_\tau T}{T} + \frac{\theta}{3} + \frac{\pi_{\mu\nu} \sigma^{\mu\nu}}{3sT} = 0, \quad (1)$$

$$\frac{\Delta_\alpha^\mu \nabla^\alpha T}{T} + D_\tau u^\mu + \frac{\Delta_\nu^\mu \nabla_\alpha \pi^{\alpha\nu}}{sT} = 0, \quad (2)$$

$$\frac{\tau_R}{sT} \left( \Delta_\alpha^\mu \Delta_\beta^\nu D_\tau \pi^{\alpha\beta} + \frac{4}{3} \pi^{\mu\nu} \theta \right) + \frac{\pi^{\mu\nu}}{sT} = -\frac{2\eta}{s} \frac{\sigma^{\mu\nu}}{T}, \quad (3)$$

where  $\nabla_\mu$  is the space-time covariant derivative,  $T$  is the local temperature,  $u^\mu$  is the 4-velocity of the fluid ( $u_\mu u^\mu = -1$ ), and  $\pi^{\mu\nu}$  is the shear-stress tensor. We use natural units  $\hbar = c = k_B = 1$ . The metric tensor in flat spacetime is  $g_{\mu\nu} = \text{diag}(-, +, +, +)$ . We further introduced the entropy density,  $s \sim T^3$ , the shear viscosity coefficient,  $\eta$ , the shear relaxation time,  $\tau_R$ , the spatial projector,  $\Delta_{\mu\nu} \equiv g_{\mu\nu} + u_\mu u_\nu$ , the comoving derivative,  $D_\tau \equiv u^\lambda \nabla_\lambda$ , the expansion rate,  $\theta \equiv \nabla_\alpha u^\alpha$ , and the shear tensor,  $\sigma^{\mu\nu} \equiv \Delta^{\mu\alpha} \Delta^{\nu\beta} \nabla_\alpha u_\beta$ , with  $\Delta^{\mu\alpha} \Delta^{\nu\beta} \equiv (\Delta^{\mu\alpha} \Delta^{\nu\beta} + \Delta^{\mu\beta} \Delta^{\nu\alpha})/2 - \Delta^{\mu\nu} \Delta^{\alpha\beta}/3$  being the double, symmetric, traceless projection operator. Even though other terms can be included in the dynamical equation for the shear-stress tensor [14, 15], for simplicity in this paper we consider only the terms present in (3).

Equation (3) contains two transport coefficients,  $\eta$  and  $\tau_R$ . In a conformal fluid, the shear viscosity coefficient is always proportional to the entropy density,  $\eta \sim s$ , while the shear relaxation time must be proportional to the inverse of the temperature,  $\tau_R \sim 1/T$ . Without loss of generality, the relaxation time is parametrized as,  $\tau_R = c\eta/(Ts)$ , where  $c$  is a constant.

We shall consider here the case in which the dynamics is boost invariant and the flow is radially symmetric, i.e.,  $T = T(\tau, r)$  and  $\pi^{\mu\nu} = \pi^{\mu\nu}(\tau, r)$ . These conditions are approximately met near mid-rapidity in ultra-central collisions at the LHC, recently measured by the ATLAS and CMS Collaborations [16, 17]. In fact, we will follow [11] and assume that the conformal fluid flow is actually invariant under  $\text{SO}(3) \otimes \text{SO}(1, 1) \otimes \text{Z}_2$ . The  $\text{SO}(3)$  piece is a subgroup of the  $\text{SO}(4, 2)$  conformal group which describes the symmetry of the solution under rotations around the beam axis and two operations constructed using special conformal transformations that replace translation invariance in the transverse plane. For more details regarding the generators of the  $\text{SO}(3)$  symmetry group of this solution, see Ref. [11]. The  $\text{Z}_2$  piece stands for invariance under  $\xi \rightarrow -\xi$ , while  $\text{SO}(1, 1)$  denotes invariance under boosts along the beam axis. In this case, the dynamical variables depend on  $\tau$  and  $r$  through the dimensionless combination [11, 12]

$$g(\tilde{\tau}, \tilde{r}) = \frac{1 - \tilde{\tau}^2 + \tilde{r}^2}{2\tilde{\tau}}, \quad (4)$$

where  $\tilde{\tau} \equiv q\tau$  and  $\tilde{r} = qr$ , with  $q$  being an arbitrary energy scale. The flow is completely determined by symmetry constraints to be [11, 12]

$$\begin{aligned} u_\tau &= -\cosh \left[ \tanh^{-1} \left( \frac{2\tilde{\tau}\tilde{r}}{1 + \tilde{\tau}^2 + \tilde{r}^2} \right) \right], \\ u_r &= \sinh \left[ \tanh^{-1} \left( \frac{2\tilde{\tau}\tilde{r}}{1 + \tilde{\tau}^2 + \tilde{r}^2} \right) \right], \\ u_\phi &= u_\xi = 0. \end{aligned} \quad (5)$$

In the following, this solution will be referred to as Gubser flow. Since the flow is known, the relativistic Euler equation (2) is automatically satisfied and, thus, only the equations for the temperature (1) and the shear-stress tensor (3) need to be solved.

The dynamical fields can be written in terms of the dimensionless variables  $\tilde{T}(g) \equiv T(\tau, r)/q$  and  $\tilde{\pi}^{\mu\nu}(g) \equiv \pi^{\mu\nu}(\tau, r)/q^4$ , which converts the partial differential equations into simple ordinary differential equations for these variables. The other variables become  $\tilde{\theta}(g) = \theta/q$ ,  $\tilde{\sigma}_{\mu\nu}(g) = \sigma_{\mu\nu}/q$ ,  $\tilde{\tau}_R = c(\eta/s)/\tilde{T}$ ,  $s = \alpha q^3 \tilde{T}^3$  and the nontrivial equations of motion considerably simplify to

$$\frac{1}{\tilde{T}(g)} D_{\tilde{\tau}} \tilde{T}(g) + \frac{1}{3} \tilde{\theta}(g) + \frac{\tilde{\pi}_{\mu\nu}(g) \tilde{\sigma}^{\mu\nu}(g)}{3\alpha \tilde{T}(g)^4} = 0, \quad (6)$$

$$\tilde{\tau}_R \left[ \Delta_\alpha^\mu \Delta_\beta^\nu D_{\tilde{\tau}} \tilde{\pi}^{\alpha\beta}(g) + \frac{4}{3} \tilde{\pi}^{\mu\nu}(g) \tilde{\theta}(g) \right] + \tilde{\pi}^{\mu\nu}(g) = -2\eta \tilde{\sigma}^{\mu\nu}(g). \quad (7)$$

We now follow [12] and perform a Weyl rescaling so then the expanding fluid in hyperbolic coordinates becomes a static fluid in some other, conveniently chosen, expanding coordinate system. The dimensionless line element in hyperbolic coordinates can be written as  $d\hat{s}^2 = -d\tilde{\tau}^2 + d\tilde{r}^2 + \tilde{r}^2 d\phi^2 + \tilde{\tau}^2 d\xi^2$ . By performing a Weyl rescaling of this metric we obtain  $d\hat{s}^2 \rightarrow d\hat{s}^2 \equiv d\tilde{s}^2/\tau^2$ , which is the metric in  $dS_3 \otimes \mathbf{R}$ , where  $dS_3$  corresponds to the 3-dimensional de Sitter space. A convenient coordinate transformation introduced in [12] takes  $d\hat{s}^2$  to  $d\hat{s}^2 = -d\rho^2 + \cosh^2 \rho d\theta^2 + \cosh^2 \rho \sin^2 \theta d\phi^2 + d\xi^2$ , where

$$\sinh \rho = -\frac{1 - \tilde{\tau}^2 + \tilde{r}^2}{2\tilde{\tau}}, \quad \tan \theta = \frac{2\tilde{r}}{1 + \tilde{\tau}^2 - \tilde{r}^2}. \quad (8)$$

In the following, we denote all fluid-dynamical variables in this coordinate system with a hat. Such generalized de Sitter coordinate is extremely convenient since it leads to a static velocity profile, i.e.,  $\hat{u}_\mu = (-1, 0, 0, 0)$ , and considerably simplifies the calculations. Since  $g = -\sinh \rho$ , the fields are only functions of  $\rho$ , i.e.,  $\hat{T} = \hat{T}(\rho)$  and  $\hat{\pi}^{\mu\nu} = \hat{\pi}^{\mu\nu}(\rho)$ . Because of the metric rescaling and the coordinate transformation  $\tilde{x}^\mu = (\tilde{\tau}, \tilde{r}, \phi, \xi) \rightarrow \hat{x}^\mu(\rho, \theta, \phi, \xi)$ , the dimensionless dynamical variables in  $dS_3 \otimes \mathbf{R}$  are related to those in hyperbolic coordinates as follows

$$u_\mu(\tilde{\tau}, \tilde{r}) = \tilde{\tau} \frac{\partial \hat{x}^\nu}{\partial \tilde{x}^\mu} \hat{u}_\nu, \quad (9)$$

$$\tilde{T}(\tilde{\tau}, \tilde{r}) = \frac{\hat{T}}{\tilde{\tau}}, \quad (10)$$

$$\tilde{\pi}_{\mu\nu}(\tilde{\tau}, \tilde{r}) = \frac{1}{\tilde{\tau}^2} \frac{\partial \hat{x}^\alpha}{\partial \tilde{x}^\mu} \frac{\partial \hat{x}^\beta}{\partial \tilde{x}^\nu} \hat{\pi}_{\alpha\beta}. \quad (11)$$

The factors of  $\tilde{\tau}$  in the transformation rules above come from the known properties of these fields under Weyl transformations [12]. For instance, since  $\pi_{\mu\nu} \rightarrow \Omega^2 \pi_{\mu\nu}$  under Weyl rescaling  $g_{\mu\nu} \rightarrow \Omega^{-2} g_{\mu\nu}$  with  $\Omega = \tilde{\tau}$ , there is a factor of  $1/\tilde{\tau}^2$  in (11). Given the dictionary between the fields in the different spaces shown above, one can solve the equations (6) and (7) in  $dS_3 \otimes \mathbf{R}$  where the fluid is static and the fields are homogeneous (i.e., they only depend on the de Sitter time coordinate  $\rho$ ) and plug in the solutions to find the fields in the standard flat space-time. This is the general strategy that we shall follow below to find solutions for the viscous relativistic fluid defined above.

### III. ISRAEL-STEWART THEORY

In this section we derive for the first time the solutions of Israel-Stewart theory in the Gubser flow regime. These solutions shall be later compared to numerical simulations of fluid dynamics. It is straightforward to work out the equations of motion for  $\hat{T}(\rho)$  and  $\hat{\pi}_\nu^\mu(\rho)$  in the generalized de Sitter coordinates. First, note that orthogonality to the flow gives  $\hat{\pi}_\rho^\mu = 0$  (where  $\mu = \rho, \theta, \phi, \xi$ ) while the tracelessness condition imposes  $\hat{\pi}_\xi^\xi = -\hat{\pi}_\theta^\theta - \hat{\pi}_\phi^\phi$ . Since the only nonzero components of the shear tensor are  $\hat{\sigma}_\xi^\xi = -2 \tanh \rho/3$ ,  $\hat{\sigma}_\theta^\theta = \hat{\sigma}_\phi^\phi = \tanh \rho/3$ , each one of the off diagonal terms of the  $\hat{\pi}_\nu^\mu$  tensor follows an independent, 1-st order linear homogeneous equation and we set their initial conditions to zero (thus, they do not contribute to the dynamics). One can show that  $\hat{\pi}_\theta^\theta$  and  $\hat{\pi}_\phi^\phi$  obey the same differential equations and, since we impose the same initial conditions for these fields,  $\hat{\pi}_\xi^\xi = -2\hat{\pi}_\theta^\theta = -2\hat{\pi}_\phi^\phi$ . We then find that the only nontrivial nonlinear equations of motion are

$$\frac{1}{\hat{T}} \frac{d\hat{T}}{d\rho} + \frac{2}{3} \tanh \rho = \frac{1}{3} \hat{\pi}_\xi^\xi(\rho) \tanh \rho, \quad (12)$$

$$\frac{c}{\hat{T}} \frac{\eta}{s} \left[ \frac{d\hat{\pi}_\xi^\xi}{d\rho} + \frac{4}{3} \left( \hat{\pi}_\xi^\xi \right)^2 \tanh \rho \right] + \hat{\pi}_\xi^\xi = \frac{4}{3} \frac{\eta}{s \hat{T}} \tanh \rho, \quad (13)$$

where  $\hat{\pi}_\xi^\xi \equiv \hat{\pi}_\xi^\xi/(\hat{T}\hat{s})$ . This variable is convenient since it is invariant under Weyl transformations. In order to derive the equations above we used that  $\hat{\theta} = 2 \tanh \rho$ .

Note that for any nonzero  $\tau$ , the value of  $\rho$  decreases with  $r$ , while for a fixed  $r$  the value of  $\rho$  increases with  $\tau$ . Thus, when  $\rho \ll 0$  one probes regions in which  $r \gg 1$ , and when  $\rho \gg 1$  one has  $\tau \gg 1$ . In this sense, we expect that physically meaningful solutions behave as  $\lim_{\rho \rightarrow \pm\infty} \hat{T}(\rho) = 0$ , i.e., at an infinite radius or time the temperature should go to zero. On the other hand, given the definition of  $\hat{\pi}_\xi^\xi$ , it is consistent to have  $\lim_{\rho \rightarrow \pm\infty} \hat{\pi}_\xi^\xi(\rho)$  finite and nonzero ( $\hat{\pi}_\xi^\xi$  is a ratio between two quantities that should vanish when  $\rho \rightarrow \pm\infty$ ).

When  $\bar{\pi}_\xi^\xi = 0$ , we have only a single equation left over for the temperature and the analytical solution is the one found in [11, 12]

$$\hat{T}_{\text{ideal}}(\rho) = \frac{\hat{T}_0}{\cosh^{2/3} \rho}, \quad (14)$$

where  $\hat{T}_0 \equiv \hat{T}_{\text{ideal}}(0)$  is a positive constant (so then  $\hat{T}_{\text{ideal}}$  is positive-definite). Using the dictionary in (10), we see that the temperature in the original hyperbolic coordinates is given by

$$T_{\text{ideal}}(\tau, r) = \frac{\hat{T}_0(2q\tau)^{2/3}}{\tau[1 + 2q^2(\tau^2 + r^2) + q^4(\tau^2 - r^2)^2]^{1/3}}, \quad (15)$$

and, at the time  $\tau_0 = 1/q$ , one finds  $T_{\text{ideal}}(\tau_0, 0) = \hat{T}_0 q$ .

The relativistic Navier-Stokes approximation to our set of equations consists in setting  $c = 0$  (i.e., the relaxation time coefficient is set to zero) while keeping  $\eta/s$  nonzero in (13). In this case,  $\bar{\pi}_\xi^\xi(\rho) = 4/(3\hat{T}) \times (\eta/s) \tanh \rho$  and the equation for  $\hat{T}$  becomes

$$\frac{d}{d\rho} \hat{T} + \frac{2}{3} \hat{T} \tanh \rho = \frac{4}{9} \frac{\eta}{s} (\tanh \rho)^2.$$

The analytical solution, previously found in [11, 12], is

$$\hat{T}_{\text{NS}}(\rho) = \frac{\hat{T}_0}{\cosh^{2/3} \rho} + \frac{4}{27} \frac{\eta}{s} \frac{\sinh^3 \rho}{\cosh^{2/3} \rho} {}_2F_1\left(\frac{3}{2}, \frac{7}{6}; \frac{5}{2}; -\sinh^2 \rho\right), \quad (16)$$

where  ${}_2F_1$  is a hypergeometric function. From the equation of motion, the condition  $\lim_{\rho \rightarrow \pm\infty} \hat{T}'_{\text{NS}}(\rho) = 0$  shows that  $\lim_{\rho \rightarrow \pm\infty} \hat{T}_{\text{NS}}(\rho) = \pm 2\eta/3s$  [11, 12]. In this case, once  $\eta/s \neq 0$ , for any given  $\tau$  there is always a value of  $r$  beyond which the temperature switches sign and becomes negative (which is very different than the ideal case in which  $\lim_{\rho \rightarrow \pm\infty} \hat{T}_{\text{ideal}} = 0$ ). This effect may be connected with the well-known causality issue (see, for instance, [18, 19]) of the relativistic Navier-Stokes equations. We shall see below that once the relaxation time coefficient is taken into account one can find a solution where  $\hat{T}$  is positive-definite and  $\lim_{\rho \rightarrow -\infty} \hat{T}(\rho) = 0$ .

Obtaining solutions of Israel-Stewart theory is more evolved, since the relaxation time in Eq. (13) cannot be set to zero, i.e.,  $\tau_R \neq 0$ . In this case  $\bar{\pi}_\xi^\xi$  obeys a differential equation (which requires an independent initial condition) and the set of equations becomes nonlinear. At the very least, it is possible to find one qualitative difference between the asymptotic solutions ( $\lim_{\rho \rightarrow \pm\infty}$ ) of Navier-Stokes and Israel-Stewart theories. If one imposes that  $\lim_{\rho \rightarrow \pm\infty} \hat{T}(\rho) = 0$  and, simultaneously,  $\lim_{\rho \rightarrow \pm\infty} d\bar{\pi}_\xi^\xi(\rho)/d\rho = 0$ , one can find the asymptotic solution for  $\bar{\pi}_\xi^\xi(\rho)$ ,  $\lim_{\rho \rightarrow \pm\infty} |\bar{\pi}_\xi^\xi(\rho)| = \sqrt{1/c}$ . Therefore, in contrast to Navier-Stokes theory solutions in which  $\lim_{\rho \rightarrow \pm\infty} \hat{T}(\rho) = 0$  are possible in Israel-Stewart theory and do happen in practice as long as  $\tau_R$  is nonzero.

There is a limit in which one can find analytical solutions for  $\hat{T}$  and  $\bar{\pi}_\xi^\xi$ . This becomes possible when the fluid is very viscous or when the temperature is very small, i.e., when  $\eta/(s\hat{T}) \gg 1$ . In this case, called here the *cold plasma limit*, the term  $\bar{\pi}_\xi^\xi$  becomes negligible in comparison to all the other terms in Eq. (13), which are all linear in  $\eta/(s\hat{T})$ . In this limit, one can directly solve the equation for  $\bar{\pi}_\xi^\xi$  to find

$$\bar{\pi}_\xi^\xi(\rho) = \sqrt{\frac{1}{c}} \tanh \left[ \sqrt{\frac{1}{c}} \left( \frac{4}{3} \ln \cosh \rho - \bar{\pi}_0 c \right) \right], \quad (17)$$

where  $\bar{\pi}_0$  is a constant and, substituting this into Eq. (12), we obtain

$$\hat{T}(\rho) = \hat{T}_1 \frac{\exp(c\bar{\pi}_0/2)}{(\cosh \rho)^{2/3}} \cosh^{1/4} \left[ \sqrt{\frac{1}{c}} \left( \frac{4}{3} \ln \cosh \rho - \bar{\pi}_0 c \right) \right]. \quad (18)$$

where  $\hat{T}_1$  is a constant. These analytical solutions are even in  $\rho$ ,  $\hat{T}$  is positive-definite, and  $\lim_{\rho \rightarrow \pm\infty} \hat{T}(\rho) = 0$  if  $4c > 1$ . Moreover, note that as long as  $c > 1$ ,  $\bar{\pi}_\xi^\xi$  is always smaller than 1 for any value of  $\rho$ , i.e., the dissipative correction to the energy-momentum tensor is always smaller than the ideal fluid contribution. In the next section,

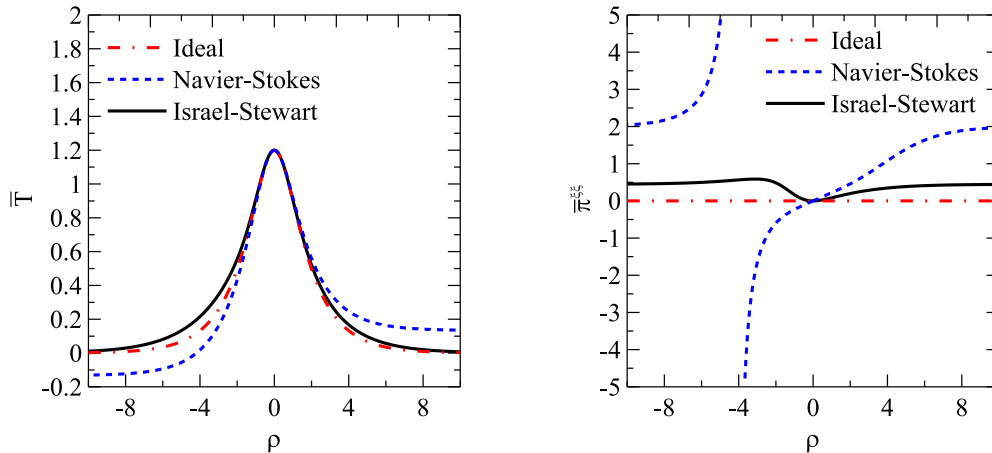


FIG. 1: Comparison between the solutions for  $\hat{T}$  (left panel) and  $\hat{\pi}_\xi^\xi$  (right panel) for  $\eta/s = 0.2$ ,  $c = 5$ , and  $\hat{T}(0) = 1.2$  found using different versions of the relativistic fluid equations. The solid black lines denote solutions of Israel-Stewart theory, results from relativistic Navier-Stokes theory are in dashed blue, while the dashed-dotted red curves correspond to the ideal fluid case.

the analytical solutions in Eqs. (17) and (18) will be compared to numerical solutions of fluid dynamics obtained with MUSIC.

We show in Fig. 1 a comparison between  $\hat{T}$  and  $\hat{\pi}_\xi^\xi$  computed for an ideal fluid, Navier-Stokes theory, and Israel-Stewart theory for  $\eta/s = 0.2$ , which is a value in the ballpark of that normally used in hydrodynamic simulations of the QGP in heavy ion collisions [20], and  $c = 5$ , which is the typical value obtained from approximations of the Boltzmann equation [21–23]. We have chosen the initial conditions for the equations such that  $\hat{T}(0) = 1.2$ , for all the cases, and, for the Israel-Stewart case,  $\hat{\pi}_\xi^\xi(0) = 0$ . We solve Eqs. (12) and (13) numerically using MATHEMATICA’s NDSolve subroutine. The Israel-Stewart theory results are shown in solid black, the Navier-Stokes results in dashed blue, and the ideal fluid result in the dashed-dotted red curve. One can see that the Israel-Stewart solution for  $\hat{T}$  is positive-definite and  $\lim_{\rho \rightarrow \pm\infty} \hat{T}(\rho) = 0$ . Moreover, viscous effects break the parity of the solutions with respect to  $\rho \rightarrow -\rho$ . Note that, as mentioned before,  $\hat{\pi}_\xi^\xi$  goes to  $\sqrt{1/c}$  when  $\rho \rightarrow \pm\infty$  in Israel-Stewart theory while for the Navier-Stokes solution this quantity diverges at  $\rho \approx -4.19$ , which is the value of  $\rho$  at which  $\hat{T}_{NS} = 0$ . We also checked that the analytical limit in Eqs. (17) and (18) matches the numerical solution for  $\eta/s = 1/(4\pi)$  [24] and  $c = 5$  when  $\hat{T}(0) \leq 0.001$ , i.e., when the temperature is extremely small.

In order to study the space-time dependence of the Israel-Stewart solutions we define  $q = 1 \text{ fm}^{-1}$  so that  $\rho = 0$  corresponds to  $\tau = 1 \text{ fm}$  and  $r = 0$ . Therefore, in standard hyperbolic coordinates,  $T(r = 0, \tau_0 = 1 \text{ fm}) = 1.2 \text{ fm}^{-1}$  and  $\hat{\pi}_\xi^\xi(r = 0, \tau_0 = 1 \text{ fm}) = 0$ . In Fig. 2 we show a comparison between the temperature profiles for Israel-Stewart theory at the times  $\tau = 1.2, 1.5, 2 \text{ fm}$ , with  $\eta/s = 0.2$ ,  $c = 5$ . Also, in the same figure we show  $\tau^2 \pi^{\xi\xi}$  as a function of the radius for the same times. The other components of the shear-stress tensor can be obtained using the dictionary in Eq. (11).

#### IV. TESTING FLUID DYNAMICS

While there are analytical and semi-analytical solutions of relativistic ideal fluid dynamics [7–10], the same is not the case for Israel-Stewart theory. This makes testing numerical algorithms that solve the equations of relativistic fluid dynamics rather problematic. Procedures such as to fix the numerical viscosity, choose the appropriate parameters for the flux limiters, among others, which strongly rely on trial and error based tests, become then highly nontrivial. Furthermore, most algorithms used to numerically solve the equations of Israel-Stewart theory were not developed for this purpose: they were developed to solve conservation laws or even Navier-Stokes theory, usually in the non-relativistic limit. In practice, most simulation codes used in heavy ion collisions have to adapt such algorithms to also solve Israel-Stewart theory. In this sense, the set of parameters that were found optimal to solve certain problems in the non-relativistic regime, such as the Riemann problem [25], might not be optimal to solve Israel-Stewart theory in the conditions produced in heavy ion collisions.

In this section, we compare numerical solutions of dissipative fluid dynamics obtained via the Kurganov-Tadmor (KT) algorithm [26] using MUSIC [13], with semi-analytical solutions of (conformal) Israel-Stewart theory in the Gubser

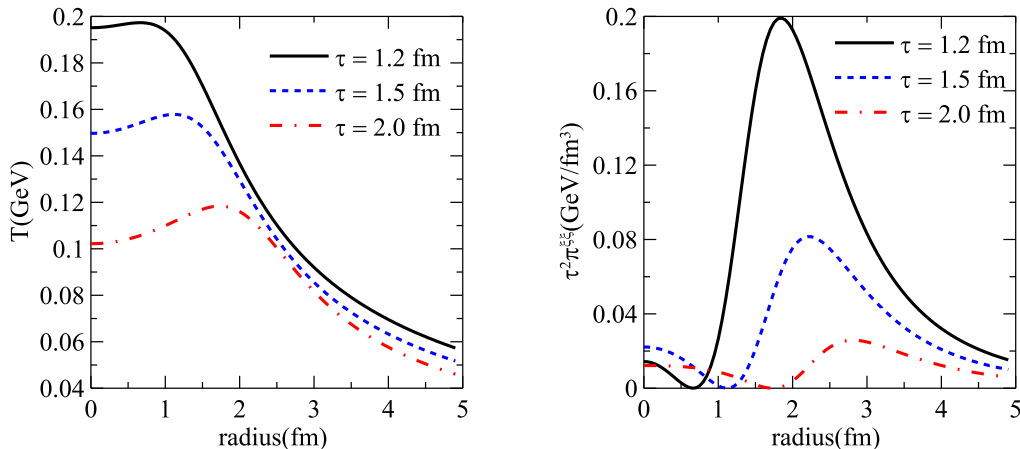


FIG. 2: Temperature and  $\tau^2 \pi^{\xi\xi}$  profiles in Israel-Stewart theory for  $\tau = 1.2$  fm (solid black curves),  $\tau = 1.5$  fm (dashed blue curves), and  $\tau = 2$  fm (dashed-dotted red curves) with  $q = 1 \text{ fm}^{-1}$ ,  $\eta/s = 0.2$ ,  $c = 5$ , and  $\hat{T}(0) = 1.2$ .

flow scenario. We show how this can be used to probe not only the quality and accuracy of the dynamical simulation but also to find the optimal value for some of the (numerical) parameters that exist in the algorithm.

In the standard version of MUSIC, the evolution equations that are solved are already those listed in Eqs. (1), (2), and (3). Therefore, the solutions calculated with MUSIC can already be compared with those of Gubser flow obtained in the previous section. For a meaningful comparison, one must initialize the numerical simulation with an initial condition constructed from the solutions of Eqs. (12) and (13) for a given initial time. In this work, we fix the initial time to be  $\tau_0 = 1$  fm. The temperature at  $\rho = 0$ , which determines the temperature at  $\tau = \tau_0$  and  $r = 0$ , is fixed to be  $T = T_0 = 1.2 \text{ fm}^{-1}$ . The shear-stress tensor at  $\rho = 0$  is initialized to be  $\pi^{\mu\nu} = 0$ . The viscosity in MUSIC is set to  $\eta/s = 0.2$  while the relaxation time is fixed to  $\tau_R = 5\eta/(\varepsilon + P)$ , i.e.,  $c = 5$ . This parametrization for the relaxation time guarantees that the fluid dynamical evolution is causal [19]. The time step and grid spacing used in the numerical simulation are  $\delta\tau = 0.005$  fm and  $\delta x = \delta y = 0.05$  fm, respectively ( $\delta\tau$ ,  $\delta x$ , and  $\delta y$  are small enough to achieve the continuum limit). We remark that in Gubser flow the values of the transport coefficients actually affect the initial condition of the fluid, since in this scheme the initial condition in hyperbolic coordinates must also be constructed by actually solving the fluid-dynamical equations in the generalized de Sitter space.

Note that MUSIC was originally designed to solve Israel-Stewart theory in 3+1-dimensions, while the Gubser flow solution assumes boost invariance. In a numerical simulation in 3+1-dimensions, boost invariance can be trivially obtained by providing an initial condition that is also boost invariant. In this situation, the solutions of fluid dynamics should maintain exact boost invariance, remaining trivial in the longitudinal direction. We checked that this does occur in the solutions obtained with MUSIC: the temperature and  $\pi^{\mu\nu}$  profiles remain (exactly) constant in the  $\xi$ -direction (e.g.,  $\pi^{\xi x}$ ,  $\pi^{x\xi}$ ,  $\pi^{\xi y}$ ,  $\pi^{y\xi}$  are exactly zero) while the longitudinal component of the velocity field is exactly zero. This is only not the case at the boundary of the grid where boost invariance is not exactly maintained due to finite size effects.

### A. Comparison to semi-analytical solution

In the following we compare the numerical solutions of MUSIC with the semi-analytical solutions of Israel-Stewart theory. Figures 3 and 4 show the spatial profiles of temperature,  $T$ , velocity,  $u^x$ , and the  $\xi\xi$ ,  $yy$ , and  $xy$  components of the shear-stress tensor,  $\pi^{\xi\xi}$ ,  $\pi^{yy}$ , and  $\pi^{xy}$ , respectively. Without loss of generality,  $T$ ,  $u^x$ ,  $\pi^{\xi\xi}$ ,  $\pi^{yy}$  are shown as a function of  $x$  in the  $y = 0$  axis, while the  $\pi^{xy}$  profile is shown as a function of  $x$  in the  $x = y$  direction. The component  $\pi^{xy}$  vanishes on the  $x, y$ -axis, which we verified also happens in MUSIC. Note that all the other components of  $\pi^{\mu\nu}$  can be obtained from the 3 components displayed, i.e.,  $\pi^{\xi\xi}$ ,  $\pi^{yy}$ , and  $\pi^{xy}$ .

One can see that the agreement between the numerical simulation and the semi-analytical solutions is very good. Only the  $xy$  component of the shear-stress tensor displayed some oscillation at late times. However, since this component is small, this oscillation is not enough to spoil the overall agreement.

We remark that such good agreement could only be obtained by adjusting the flux limiter used in the KT algorithm. Flux limiters are employed in MUSCL scheme algorithms, such as the KT algorithm, to control artificial oscillations that usually occur when using higher order discretization schemes for spatial derivatives. Such spurious oscillations



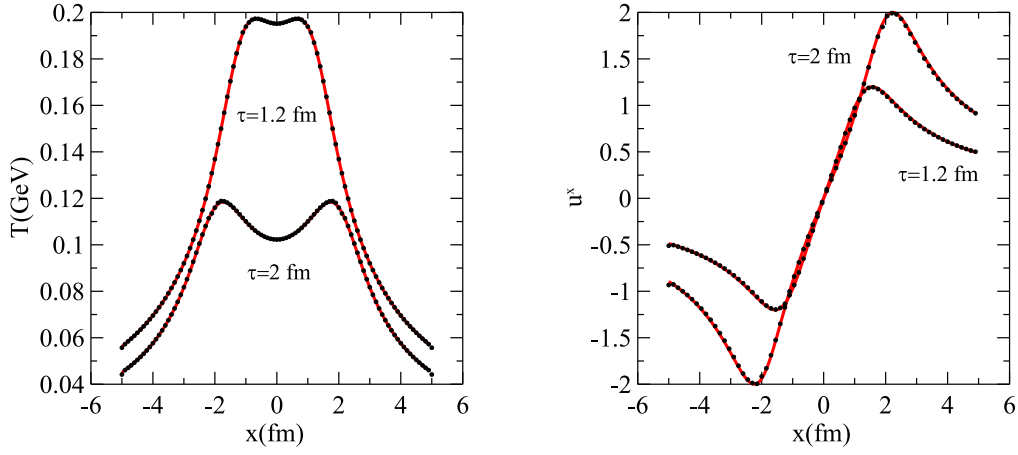


FIG. 3: Comparison between the solutions for temperature (left panel) and the  $x$ -component of the 4-velocity (right panel) from Gubser flow and MUSIC (numerical), as a function of  $x$ . In this plot  $\eta/s = 0.2$  and  $\tau_R T = 5\eta/s$ . The solid lines denote the semi-analytic solution while the points denote solutions obtained from MUSIC.

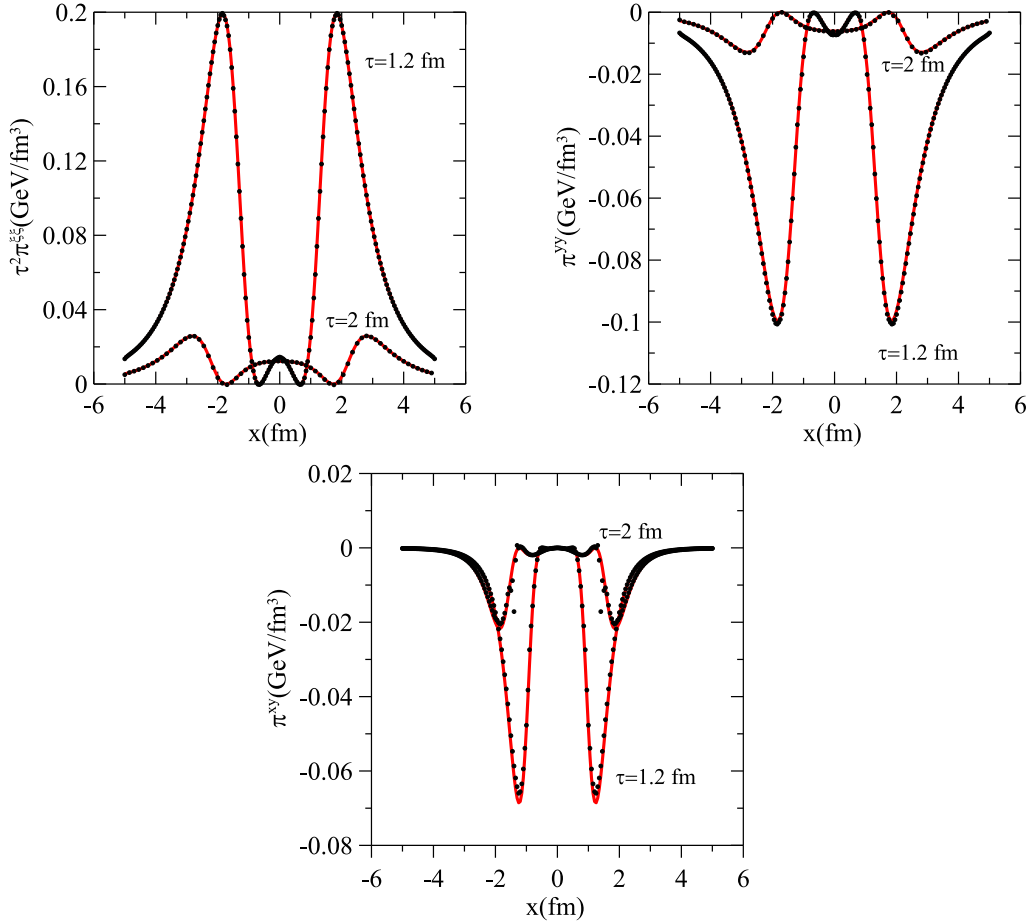


FIG. 4: Comparison between the solutions for the  $\xi\xi$  (left panel),  $yy$  (right panel), and  $xy$  (lower panel) components of the shear-stress tensor from Gubser flow and MUSIC (numerical), as a function of  $x$ . In this plot  $\eta/s = 0.2$  and  $\tau_R T = 5\eta/s$ . The solid lines denote the semi-analytic solution while the points denote solutions obtained from MUSIC.

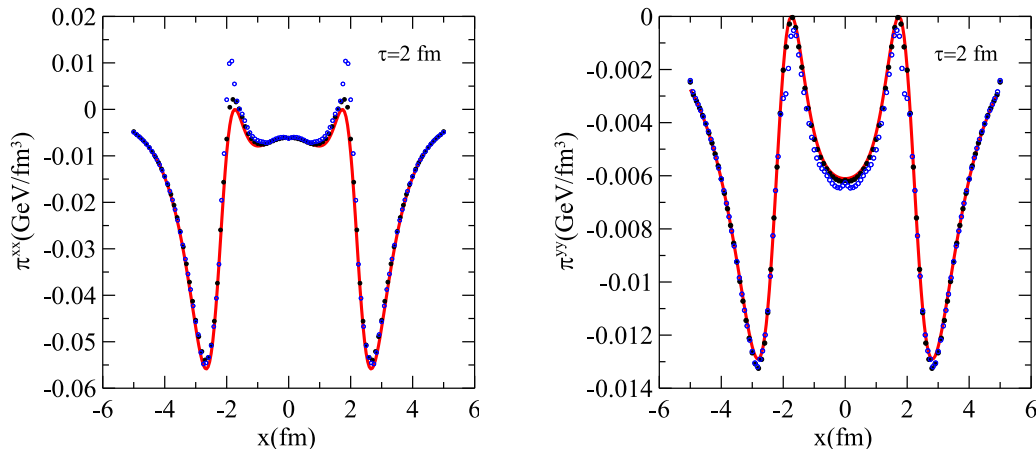


FIG. 5: Numerical solutions of MUSIC obtained with  $\theta = 1.1$  (open circles) for the  $xx$  (left panel) and  $yy$  (right panel) components of the shear-stress tensor. The full circles correspond to the solutions obtained with  $\theta = 1.8$  and the solid lines correspond to the semi-analytic solution.

are known to appear when resolving shock problems, solutions with discontinuities in density profiles or velocity field, or even when describing systems which display high gradients, such as the system created in relativistic heavy ion collisions. Since dissipative effects originate mainly from space-like gradients of the velocity field, flux limiters are essential in order to obtain a precise numerical solution of dissipative fluid dynamics.

Currently, there are several flux limiter algorithms available and many others still being developed. In MUSIC, the van Leer minmod filter is used [13]. In this case, the gradients of currents and fluxes are controlled according to a free parameter  $\theta$ , which may vary from  $\theta = 1$  (most dissipative) to  $\theta = 2$  (least dissipative). The optimal value of  $\theta$  can vary case by case and is usually fixed by trial and error; in previous work, MUSIC was run with  $\theta = 1.1$ . However, the agreement displayed in Figs. 3 and 4 is only obtained by choosing a larger value,  $\theta = 1.8$ , corresponding to the less diffusive case. The solutions of the temperature and velocity fields are not very sensitive to changes in the flux limiter scheme. On the other hand, the solutions of the shear-stress tensor do depend on the choice of this numerical parameter. In Fig. 5 we show the numerical solutions of MUSIC obtained with  $\theta = 1.1$  (open circles) for the  $xx$  and  $yy$  components of the shear-stress tensor, which are the components most sensitive to this parameter. These solutions are compared with those of  $\theta = 1.8$  (full circles) and the semi-analytical solutions (solid line). One can see that when  $\theta = 1.1$  the agreement becomes worse, demonstrating the usefulness of the semi-analytic solution found in this paper in testing the algorithm. It should be noted that, if a flux limiter is not employed at all, it is not possible to properly describe the Gubser flow solutions of Israel-Stewart theory.

### B. Comparison to analytical solution

In the previous section, we showed that an analytical solution for Israel-Stewart theory can be found in the limit of extremely large viscosity or, equivalently, of extremely small temperatures (cold plasma limit). Note that this analytical solution is no longer an approximation if the term  $\pi^{\mu\nu}$  is removed from Israel-Stewart theory. That is, if one solves the equation,

$$\frac{\tau_R}{sT} \left( \Delta_\alpha^\mu \Delta_\beta^\nu D_\tau \pi^{\alpha\beta} + \frac{4}{3} \pi^{\mu\nu} \theta \right) = -\frac{2\eta}{s} \frac{\sigma^{\mu\nu}}{T}, \quad (19)$$

instead of Eq. (3).

The solution of this equation no longer relaxes to Navies-Stokes theory. However, it can still be used to test algorithms that solve relativistic fluid dynamics. The same algorithm that solves Israel-Stewart theory should also be able to solve the above equation of motion and this can be used as an independent and powerful test of a given numerical approach. Furthermore, the term  $\pi^{\mu\nu}$  is rather simple and does not demand much work to be removed.

As already mentioned, in this case the solution of the theory in de Sitter space can be found analytically, see Eqs. (18) and (17). We numerically solved Eqs. (1), (2), and (19) using MUSIC by subtracting the aforementioned term, using the same initial condition described before. The comparison is showed in Figs. 6 and 7, which show the spatial



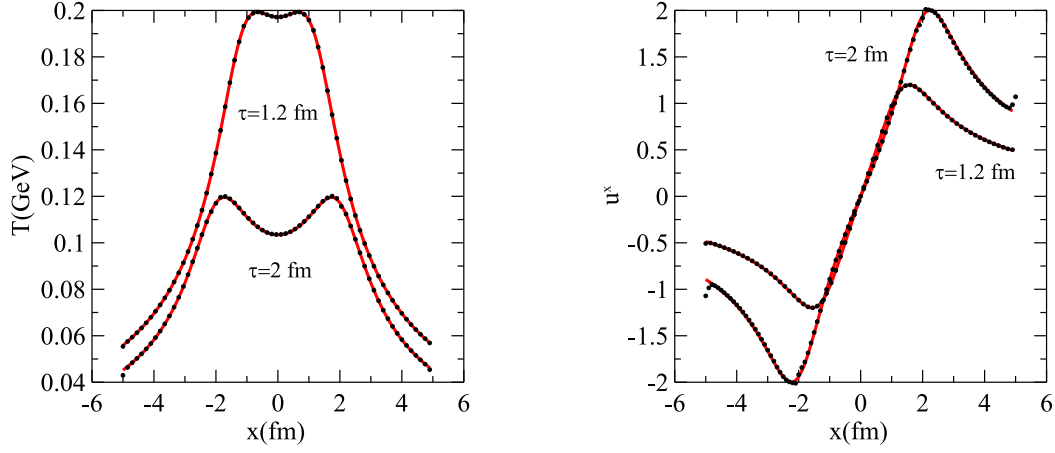


FIG. 6: Comparison between the solutions for temperature (left panel) and the  $x$ -component of the 4-velocity (right panel) from Gubser flow and MUSIC (numerical), as a function of  $x$ . In this plot  $\eta/s = 0.2$  and  $\tau_R T = 5\eta/s$ . The solid lines denote the analytic solution while the points denote solutions obtained from MUSIC.

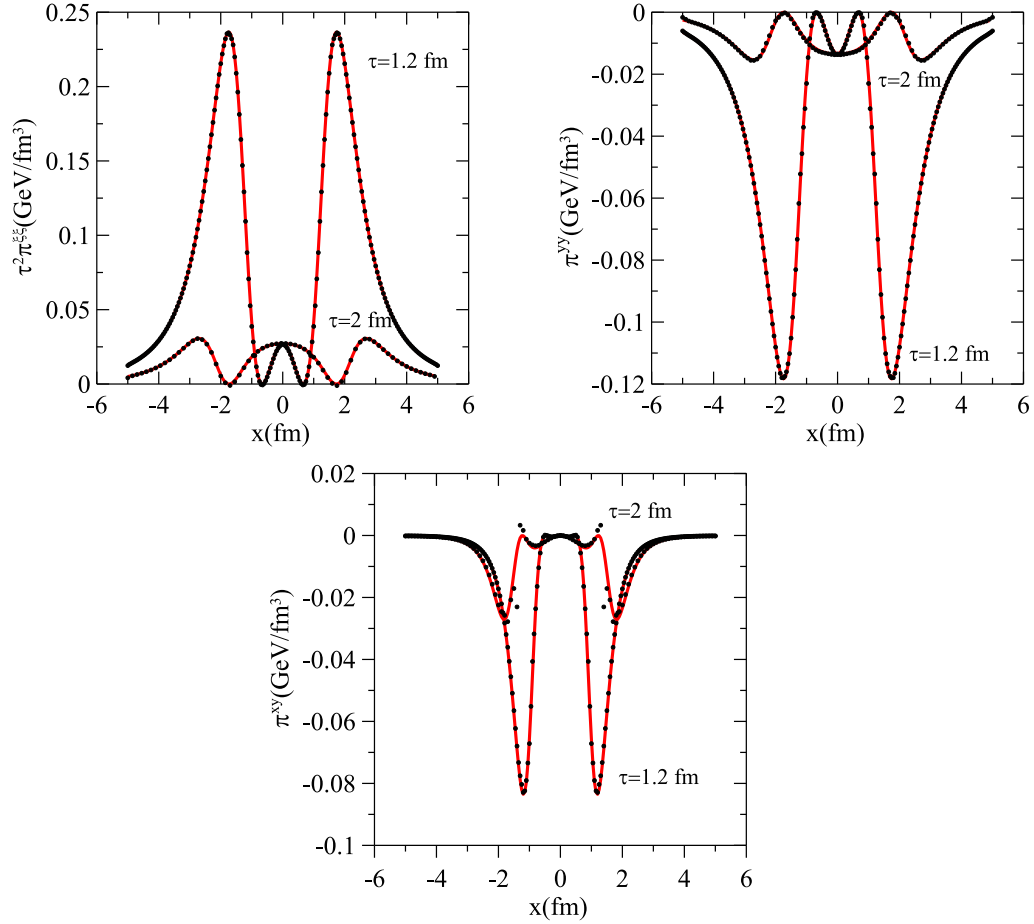


FIG. 7: Comparison between the solutions for the  $\xi\xi$  (left panel),  $yy$  (right panel), and  $xy$  (lower panel) components of the shear-stress tensor from Gubser flow and MUSIC (numerical), as a function of  $x$ . In this plot  $\eta/s = 0.2$  and  $\tau_R T = 5\eta/s$ . The solid lines denote the analytic solution while the points denote solutions obtained from MUSIC.

profiles of  $T$ ,  $u^x$ ,  $\pi^{\xi\xi}$ ,  $\pi^{yy}$ , and  $\pi^{xy}$ . The solid lines correspond to the analytical solutions while the points correspond to the numerical solutions of Eq. (19) obtained with MUSIC.

Note that the level of agreement is the same as before. The solutions in hyperbolic coordinate even appear to be qualitatively the same, containing the same general structures as the full solutions. However, from a practical point of view, the above solutions are very convenient to test a code since they are already cast in the form of functions and can be written directly into the code.

## V. CONCLUSIONS

We have presented the first analytical and semi-analytical solutions of a radially expanding viscous conformal fluid that follows relaxation-type equations such as the Israel-Stewart equations. The  $SO(3) \otimes SU(1,1) \otimes Z_2$  invariant solutions for the temperature, shear stress tensor, and flow discussed here can be used to test the existing numerical algorithms used to solve the equations of motion of viscous relativistic fluid dynamics in ultrarelativistic heavy ion collision applications.

We further demonstrated how the solutions derived in this paper can be used to optimize the numerical algorithm of a well known hydrodynamical code, fixing numerical parameters that can only be determined by trial and error. The MUSIC simulation code was shown to produce results that are in good agreement with the analytic and semi-analytic solutions of Israel-Stewart theory undergoing Gubser flow.

Also, once the temperature and shear-stress tensor profiles are known, one can use this information for instance to study the energy loss of hard probes in a radially expanding and viscous QGP scenario [27, 28]. Another interesting aspect that could be studied would be the propagation of small disturbances [12, 29] on the expanding IS fluid background found here in which the temperature is positive definite throughout the whole dynamical evolution (which is not the case in the Navier-Stokes solution). Moreover, it would be interesting to see if the solutions found here for the conformal Israel-Stewart equations correspond to a black hole configuration in an asymptotically  $AdS_5$  geometry, as it is the case for the NS equations at zero chemical potential [30].

The authors acknowledge many useful exchanges with B. Schenke, and are grateful to I. Kozlov, J.-F. Paquet, D. H. Rischke, J.-B. Rose, and G. Vujanovic for discussions. This work was funded in part by Fundação de Amparo à Pesquisa do Estado de São Paulo (FAPESP), in part by Conselho Nacional de Desenvolvimento Científico e Tecnológico (CNPq), and in part by the Natural Sciences and Engineering Research Council of Canada. G. S. Denicol acknowledges the support of a Banting fellowship provided by the Natural Sciences and Engineering Research Council of Canada.

- 
- [1] M. Gyulassy and L. McLerran, Nucl. Phys. A **750**, 30 (2005) [nucl-th/0405013].
  - [2] U. W. Heinz and R. Snellings, arXiv:1301.2826 [nucl-th].
  - [3] C. Gale, S. Jeon, and B. Schenke, Int. J. Mod. Phys. A **28**, 1340011 (2013) [arXiv:1301.5893].
  - [4] W.A. Hiscock and L. Lindblom, Ann. Phys. (N.Y.) **151**, 466 (1983); Phys. Rev. D **31**, 725 (1985); Phys. Rev. D **35**, 3723 (1987); Phys. Lett. A **131**, 509 (1988); Phys. Lett. A **131**, 509 (1988).
  - [5] W. Israel, Annals Phys. **100**, 310 (1976); W. Israel and J. M. Stewart, Annals Phys. **118**, 341 (1979).
  - [6] L. D. Landau and E. M. Lifshitz, *Fluid Mechanics*, Second Edition: Volume 6 (Course of Theoretical Physics), Butterworth-Heinemann, 1987.
  - [7] J. D. Bjorken, Phys. Rev. D **27**, 140 (1983).
  - [8] T. Csorgo, F. Grassi, Y. Hama and T. Kodama, Phys. Lett. B **565**, 107 (2003) [nucl-th/0305059].
  - [9] T. Csorgo, L. P. Csernai, Y. Hama and T. Kodama, Heavy Ion Phys. A **21**, 73 (2004) [nucl-th/0306004].
  - [10] T. Csorgo, M. I. Nagy and M. Csanad, Phys. Lett. B **663**, 306 (2008) [nucl-th/0605070].
  - [11] S. S. Gubser, Phys. Rev. D **82**, 085027 (2010) [arXiv:1006.0006 [hep-th]].
  - [12] S. S. Gubser and A. Yarom, Nucl. Phys. B **846**, 469 (2011) [arXiv:1012.1314 [hep-th]].
  - [13] B. Schenke, S. Jeon and C. Gale, Phys. Rev. C **82**, 014903 (2010) [arXiv:1004.1408 [hep-ph]]; Phys. Rev. Lett. **106**, 042301 (2011) [arXiv:1009.3244 [hep-ph]]; Phys. Rev. C **85**, 024901 (2012) [arXiv:1109.6289 [hep-ph]].
  - [14] R. Baier, P. Romatschke, D. T. Son, A. O. Starinets and M. A. Stephanov, JHEP **0804**, 100 (2008) [arXiv:0712.2451 [hep-th]].
  - [15] J. Noronha and G. S. Denicol, arXiv:1104.2415 [hep-th].
  - [16] G. Aad *et al.* [ATLAS Collaboration], Phys. Rev. C **86**, 014907 (2012) [arXiv:1203.3087 [hep-ex]].
  - [17] [CMS Collaboration], CMS-PAS-HIN-12-011.
  - [18] G. S. Denicol, T. Kodama, T. Koide and P. Mota, J. Phys. G **35**, 115102 (2008) [arXiv:0807.3120 [hep-ph]].
  - [19] S. Pu, T. Koide and D. H. Rischke, Phys. Rev. D **81**, 114039 (2010) [arXiv:0907.3906 [hep-ph]].
  - [20] M. Luzum and J. -Y. Ollitrault, Nucl. Phys. A904-905 **2013**, 377c (2013) [arXiv:1210.6010 [nucl-th]].
  - [21] G. S. Denicol, T. Koide and D. H. Rischke, Phys. Rev. Lett. **105**, 162501 (2010) [arXiv:1004.5013 [nucl-th]].

- [22] G. S. Denicol, J. Noronha, H. Niemi and D. H. Rischke, Phys. Rev. D **83**, 074019 (2011) [arXiv:1102.4780 [hep-th]].
- [23] G. S. Denicol, H. Niemi, E. Molnar and D. H. Rischke, Phys. Rev. D **85**, 114047 (2012) [arXiv:1202.4551 [nucl-th]].
- [24] P. K. Kovtun, D. T. Son and A. O. Starinets, Phys. Rev. Lett. **94**, 111601 (2005) [hep-th/0405231].
- [25] D. H. Rischke, Y. Pursun and J. A. Maruhn, Nucl. Phys. A **595**, 383 (1995) [Erratum-ibid. A **596**, 717 (1996)]; D. H. Rischke, In \*Cape Town 1998, Hadrons in dense matter and hadrosynthesis\* 21-70 [nucl-th/9809044].
- [26] A. Kurganov and E. Tadmor, Journal of Computational Physics **160**, 214 (2000); R. Naidoo and S. Baboolal, Future Gener. Comput. Syst. **20**, 465 (2004).
- [27] B. Betz and M. Gyulassy, arXiv:1305.6458 [nucl-th].
- [28] B. Schenke, C. Gale and S. Jeon, Phys. Rev. C **80**, 054913 (2009) [arXiv:0909.2037 [hep-ph]].
- [29] P. Staig and E. Shuryak, Phys. Rev. C **84**, 044912 (2011) [arXiv:1105.0676 [nucl-th]].
- [30] S. Bhattacharyya, V. E. Hubeny, S. Minwalla and M. Rangamani, JHEP **0802**, 045 (2008) [arXiv:0712.2456 [hep-th]].